Static and Dynamic Characterization of Cellulose Nanofibril Scaffold-Based Composites

Issam I. Qamhia,[a] Ronald C. Sabo,[b] and Rani F. Elhajjar [a,*]

The reinforcement potential of novel nanocellulose-based scaffolding reinforcements composed of microfibrils 5 to 50 nm in diameter and several microns in length was investigated. The cellulose nanofibril reinforcement was used to produce a three-dimensional scaffolding. A hybrid two-step approach using vacuum pressure and hot pressing was used to integrate the nanocellulose reinforcements in a liquid molding process with an epoxy resin to manufacture composites containing fiber volume contents ranging from 0.6% to 7.5%. The mechanical properties were studied using three-point bending. The Shore-D hardness test and differential scanning calorimetry (DSC) were used to investigate the curing response and its relation to the mechanical properties. Dynamic mechanical analysis (DMA) with a three-point bend setup was used to investigate the viscoelastic behavior of the nanocellulose composite samples at various temperatures and dynamic loadings. The results using the proposed liquid resin manufacturing method for processing the nanocellulose composites showed an increased modulus and a lower strain-to-failure compared to neat resin. Dynamic testing showed a trend of lower tan delta peaks and a reduction in the glass transition temperature with the addition of nanocellulose reinforcement.

*Contact information: a: College of Engineering & Applied Science, University of Wisconsin, Milwaukee, Wisconsin 53211, USA; b: USDA Forest Products Laboratory, Madison, Wisconsin 53726, USA; * Corresponding author: elhajjar@uwm.edu*

INTRODUCTION

Nanocellulose-based reinforcements constitute a relatively new class of naturally sourced reinforcements. Cellulose nanomaterials have high mechanical properties and are derived from natural resources, and there is thus significant interest in incorporating them into composite materials. The advantages of these materials include good transparency, dimensional stability, and good barrier properties (Iwamoto *et al.* 2005, 2007; Nogi *et al.* 2005, 2006, 2009; Nogi and Yano 2008, 2009; Nogia *et al.* 2006; Okahisa *et al.* 2009; Sabo *et al.* 2012). Cellulose nanocomposites can offer transparency due to the small cross-section of the nanofibers, which does not result in light scattering, even at high reinforcement ratios. Biodegradable cellulose nanocomposites are a potential material for replacing synthetic materials in the food packaging industry, as they can be used to improve the mechanical and barrier properties of bio-polymers and also provide antimicrobial activity, enzyme immobilization, and biosensing (Azeredo 2009).

Nanofibrillated cellulose (NFC) or cellulose nanofibrils (CNFs) are fibrillated cellulose with a nano-scale structure and are typically created by some combination of chemical (Saito *et al.* 2009; Jonoobi *et al.* 2009), enzymatic (Pääkkö *et al.* 2007; Qing *et*

bioresources.com

al. 2013), and/or mechanical treatments of lignocellulosic materials, such as wood. CNFs have a complex structural hierarchy with fibril bundles of about 5 to 50 nm in diameter and up to several microns in length (Moon *et al.* 2011). The strong tendency of cellulosic nanomaterials to form hydrogen bonds can lead to challenges in re-dispersing them if they are dried; this property can also result in fairly strong and stiff films that can be used in laminated composites (Sehaqui *et al.* 2012). Cellulose nanomaterials are very hydrophilic (Qing *et al.* 2012), which can create difficulties in dispersing them and bonding them to some thermosetting polymers due to swelling during composite manufacture. Thermosetting composites can be cured with low or no heat applied, which can be advantageous because nanocellulose has limited thermal stability. The curing in thermosets may be initiated through heat, radiation, or a chemical reaction (*e.g.,* a two-part epoxy). Uncured thermosetting materials can have low viscosities, which is a critical feature in the construction of composites that allows for infiltration and wetting of the fibers. Distributed or particulate composites based on nanocellulose benefit from inter-actions with the resin and the relatively high aspect ratios of the cellulose particles or fibers. Ruiz *et al.* (2000) manufactured cellulose nanofibril composites with aqueous suspensions of epoxy. The CNFs displayed large aspect ratios and an ability to associate by means of hydrogen bonds.

The effect of fiber content on the mechanical and thermal expansion properties of CNFs biocomposites has also been reported (Nakagaito and Yano 2008). A linear increase in the Young's modulus was observed at fiber contents up to 40% wt., using a phenolic resin. The results also showed a correlation between the coefficient of thermal expansion (CTE) relative to fiber content, indicating the effective reinforcement attained by the CNFs. In another example, Ruiz *et al.* (2000) found that adding CNFs up to about 2% in an epoxy resin increased the mechanical properties, but further addition of CNFs led to agglomeration and reduced the thermal and mechanical properties. The pressing method has been found to be the most common processing technique in the literature for producing thermosetting composites with CNFs reinforcements. Essentially, no detailed reports of resin infiltrating into CNF scaffolds or aerogels have been reported in the literature. This study examined the reinforcement of novel nanocellulose-based reinforcements manufactured to produce a three-dimensional scaffolding. A two-step approach using vacuum pressure and hot pressing was used to integrate scaffold-type nanocellulose reinforcements in a low-viscosity epoxy resin. Dynamic mechanical analysis (DMA) and differential scanning calorimetry (DSC), as well as hardness and bending tests, were used to characterize the nanocellulose composites.

MATERIALS AND METHODS

Production of CNF Scaffolds

TEMPO-oxidized cellulose nanofibrils (Fig. 1) used in this study were prepared following the work reported by Saito *et al.* (2009). The TEMPO process was used because it yields CNF scaffolds with more integrity and less agglomeration compared to other methods. Fully bleached kraft eucalyptus pulp fibers were carboxylated using 2,2,6,6-tetramethylpiperidine-1-oxyl (TEMPO), sodium chlorite, and sodium hypo-chlorite as the reactants at 60 °C for 48 h. TEMPO-oxidized pulp fibers were then washed thoroughly using distilled water and homogenized in a disk refiner to break apart the fibril bundles. The fiber slurry was diluted to facilitate the separation of coarse and

fine fractions by centrifugation at 120,000 m/s^2, and the coarse fraction was rejected. The nanofiber suspension was concentrated to approximately 0.6% solids content using ultrafiltration. A final clarification step was performed, in which the nanofiber suspension was passed once through an M-110EH-30 Microfluidizer (Microfluidics, Newton, MA) with 200- and 87-µm chambers in series.

The carboxylate content of reacted pulp fibers was measured *via* titration based on the TAPPI Test Method T 237 cm-98 (TAPPI 1998); the TEMPO-modified fibers were found to contain 0.65 mmol COONa per gram of pulp.

The scaffolds (Fig. 2) were created by freeze-drying diluted suspensions of cellulose nanofibrils in a Vir Tis model 36DX84 tray-type freeze drier. Chilled suspensions were placed in trays, and the setpoint of the freeze drier was -20 °C. The condenser removed approximately 5 to 10 L of water per day, and the process was stopped once the material was dry, as indicated by the rapid changes in the operating pressure and temperature of the chamber.
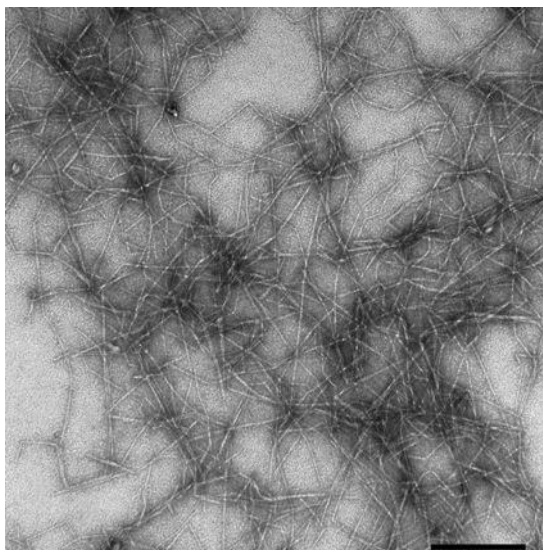
Fig. 1. Transmission electron micrograph of cellulose nanofibrils. The scale bar is 200 nm.
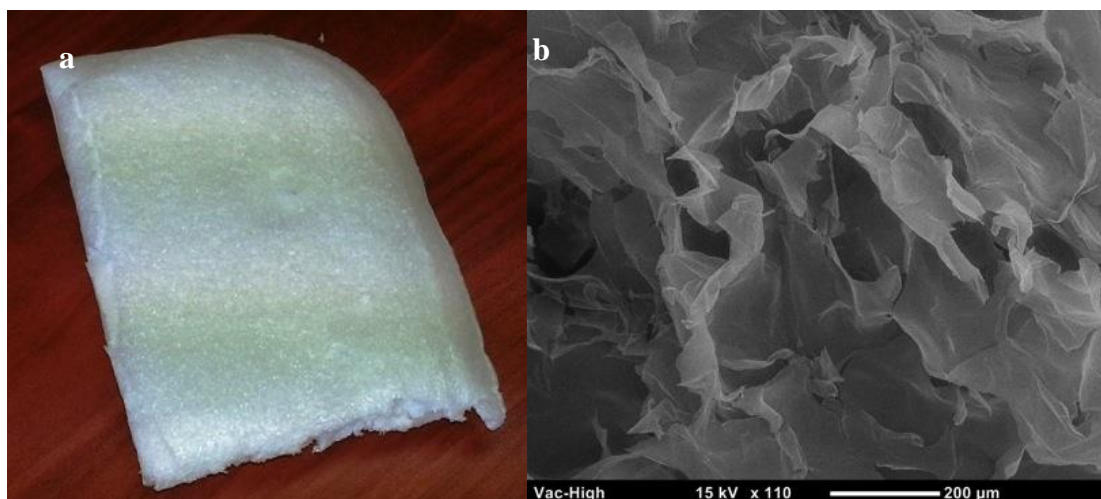
Fig. 2. Photograph (a) and scanning electron micrograph (b) of cellulose nanofibril scaffolds

PEER-REVIEWED ARTICLE

bioresources.com

Morphological Characterization of the CNF Scaffolds and Composites

Transmission electron microscope (TEM) images of CNFs were acquired using a Philips CM-100 TEM, operated at 100 kV using an SIA L3C 4-2Mpixel CCD camera (Scientific Instruments and Application, Duluth, GA). These CNFs had an average diameter of 5 to 7 nm with lengths on the order of micrometers, and they were further characterized by the authors elsewhere (Qing *et al.* 2013).

Composite Fabrication

Composites were fabricated from the nanocellulose scaffolds with the aid of a thermosetting epoxy resin. The composites were manufactured using a low-viscosity epoxy system (*Embed-It™* Low Viscosity Epoxy; Polysciences Inc., Warrington, Pennsylvania, USA) with a viscosity of 65 cPs when mixed and a long working time (> 48 h if no heat is applied). Using the low-viscosity epoxy, two experimental fabrication methods were used with the nanocellulose scaffolds. The first method was vacuum-assisted casting followed by heat curing (VAC-H). For this fabrication technique, nanocellulose scaffolds were placed in an epoxy resin bath under a vacuum pressure of 635.0 mm Hg (25 in. Hg) for 60 ± 2 min. After this step, the mold was placed over a heated plate to cure overnight (15 to 16 h) at a temperature of 70 °C. The resulting composites were polished against a 320 SiC abrasive disc with a 250 rpm platen speed to ensure flat surfaces and to remove excess epoxy. The second composite fabrication technique involved vacuum-assisted casting followed by hot pressing (VAC-HP). In this method, the vacuum-assisted casting was performed in the same manner as before. However, for the resin curing, a press-claving method was used instead of the hot plate. The curing procedure consisted of increasing the temperature from 27 °C at a rate of 6 °C/min. The temperature was then held at 120 °C for 210 min then allowed to decrease at a rate of 6 °C/min to 27 °C. During the curing, a 445-N compressive force, equivalent to approximately 38 kPa (5.5 psi) pressure, was applied to the composite scaffolds to increase fiber volume fraction and reduce porosity.

Mechanical, Thermal, and Viscoelastic Characterization

Sample hardness was measured using a Shore-D hardness tester. A hardness value of 70 or above generally indicates a fully cured sample. This was subsequently confirmed with differential scanning calorimetry (DSC) measurements. DSC was performed on cured specimens extracted from the pure epoxy and nanocellulose-reinforced specimens prepared by both the VAC-H and VAC-HP methods. DSC was used to investigate the physical and chemical changes that occur when the nanocellulose is incorporated into the epoxy resin. Three-point bending tests were performed on the pure resin and nanocellulose-embedded specimens. The sample dimensions and test setup were chosen to comply with the recommendations of the ASTM D790-10 test standard for flexural testing (ASTM 2010). The simply supported beam had a 50-mm span with a 10-mm overhang. Samples were supported on 11-mm-diameter supports, and the loads were applied at mid-span. Tests were carried out using an electromechanical loading machine having a maximum loading capacity of 97.8 kN with a 2.2-kN-capacity load cell. The specimens were loaded at a displacement-controlled rate of 1.3 mm/min. Simultaneous measurements for the load, displacement, and time were recorded. The flexural stresses and strains were determined with a strength of materials approach using the relationships of ASTM D790-10 (ASTM 2010). A scanning electron microscope (SEM) was used on

Qamhia *et al.* (2014). "Cellulose nanofibril scaffolds," *BioResources* 9(1), 381-392.   384

the fractured surfaces of the CNF/epoxy composites to investigate the failure morphology (SM-300 SEM; TopCon, Japan).

The effect of nanocellulose reinforcement on the viscoelastic properties was examined using dynamic mechanical analysis. The study was conducted on a Q800 DMA TA instrument (TA instruments, New Castle, Delaware, USA). A three-point bending mode with a controlled strain mode of 15 μm (displacement) was used. Pure resin samples and samples of nanocellulose/epoxy with different fiber volume fractions prepared with the VAC-HP method were tested at a constant frequency of 1.0 Hz. A temperature range of 0 to 120 °C and a heating rate of 5 °C/min were chosen. The tested samples were approximately 35 x 12 to 15 x 1.5 to 2.0 mm in length, width, and thickness, respectively. The supported span width was 20 mm. The test parameters were chosen to comply with the general recommendations of the ASTM D4065-12 and ASTM D5023-07 standards (ASTM 2007).
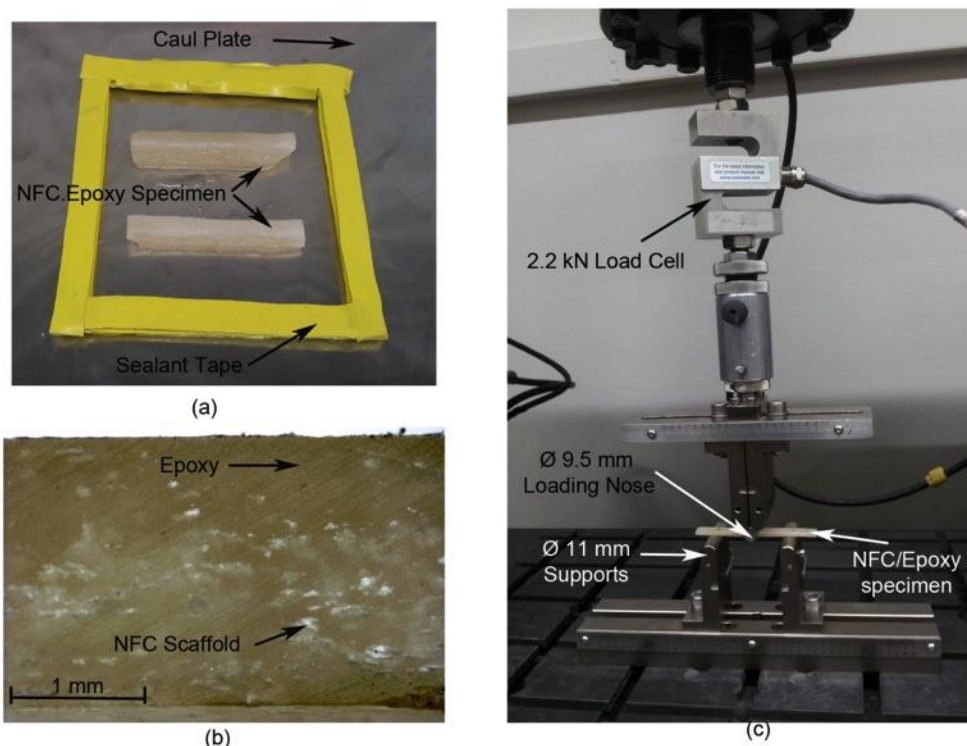
Fig. 3. Test specimens and experimental setup: (a) prior to resin addition, (b) cross-section post-cure and (c) experimental three-point bending setup

RESULTS AND DISCUSSION

The curing of the resin system was found to be dependent on the process parameters. This resin system was chosen because initial trials with a relatively high-viscosity (650 cPs at 25 °C) epoxy resin (Super Sap 100; Entroy Resins, Hayward, CA, USA) showed a poor infusion, with a void content exceeding 60% for most of the prepared samples. The use of the low viscosity resin reduced the void content to 3.5 to 9% for composites prepared by the VAC-H method and to 0.7 to 4% for composites prepared by VAC-HP. Additionally, the VAC-HP method enabled higher cellulose

content in the composites (up to 7.5% by volume) as compared to the VAC-H method. The VAC-H method produced composites with 0.7 to 1% nanocellulose content. The better composite properties in terms of lower void content and higher nanocellulose content observed for the composites prepared by VAC-HP are believed to result from the pressing effect, which eases the flow of the resin and compact the cellulose into a denser packing arrangement. The specimens prepared using this method showed a significantly higher elastic modulus and strength compared to specimens prepared with the VAC-H method (NC_VAC-H). The VAC-HP process resulted in a 15% average increase in the modulus compared to neat resin for reinforcement levels of 5 to 7.5%. The strain-to-failure decreased from 5.5 to 6% in the unreinforced specimens to 2.3 to 3.0% in the CNF/epoxy composites (Fig. 4). The maximum bending stress of the CNF-reinforced composites (NC_VAC-HP) was found to be less than that of the neat epoxy samples (EP_VAC-HP). However, the CNF-reinforced composites did not show much plastic deformation compared to the neat resin, so the yield strengths for the neat and CNF-reinforced samples were similar.
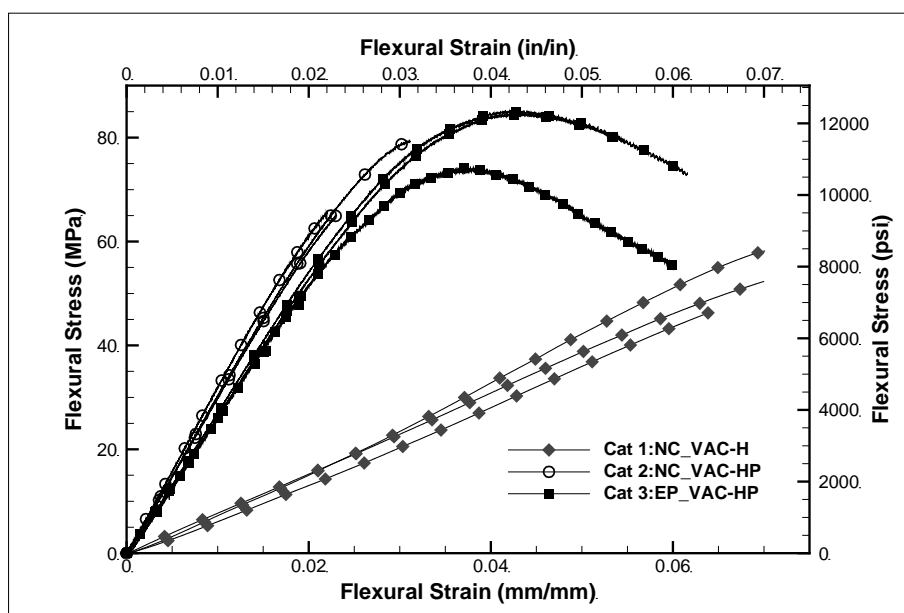
Fig. 4. The stress-strain response of pure epoxy and CNF/epoxy specimens using both methods

The results from this research are summarized in Table 1. Previous work using films as reinforcements at 1 to 6% loadings in epoxy resulted in modest increases in the tensile modulus (Masoodi *et al.* 2012), which was similar to the increase in bending modulus seen in the present work with CNF scaffolds. However, in the case of films, delamination was observed between the CNF and epoxy layers. Porous scaffolds are expected to improve the adhesion and entanglement between the cellulose and the epoxy and prevent such delaminations.

Figure 5 shows the results from DSC analysis. Using DSC, it is possible to determine the degree of curing and glass transition temperature (T_g) of composite materials. The results from the VAC-H technique showed an exothermic peak for the CNF-reinforced specimens at a temperature of 170 °C. The peak was non-existent for pure epoxy specimens prepared by both techniques.

Table 1. Comparison of CNF Composites to Unreinforced Polymer

Resin	Nano-cellulose Form	Process	Strength (MPa)	Initial Elastic modulus (GPa)	Strain-to-failure (%)
Epoxy	No CNFs	Vacuum/ Press	75-85	2.43-2.56	5.5-6
Epoxy	CNF Scaffolding	Vacuum/ Press	67-80	2.79-3.03	2.2-3.0
Epoxy	CNF Scaffolding	Vacuum/ Heat	48-60	0.67-0.82	6.5-7.0

For the CNF/epoxy composites using the VAC-HP method, the exothermic peak was not observed. A clear drop in heat flow was observed for pure epoxy at 265 °C. A change in slope at the same temperature was observed for nanocellulose specimens, indicating a similar behavior (Fig. 5). The authors believe that this drop in heat flow was not due to a glass transition, but might have been due to the degradation of the resin. DSC experiments were performed for pure resin samples and nanocellulose-reinforced composites with different fiber volume fractions prepared by the VAC-HP method at lower temperatures, and a clear T_g was observed at a temperature of around 60 °C for both categories (Fig. 6). The nanocellulose did not appear to significantly affect the glass transition temperature of the composite. The glass transition temperature was also investigated with DMA. These results revealed the importance of proper resin curing to the properties of the composites. No exothermic peaks were observed for samples prepared by VAC-HP compared to those obtained when using the standard curing procedure. The conditions in the VAC-HP resulted in complete curing, as seen in both the improved mechanical properties and the disappearance of the exothermic peak in the DSC results. The DSC results showed an exothermic peak at 170 °C in the nanocellulose composites only when the resin was not cured properly. This peak was not seen for the materials processed using the VAC-HP method.
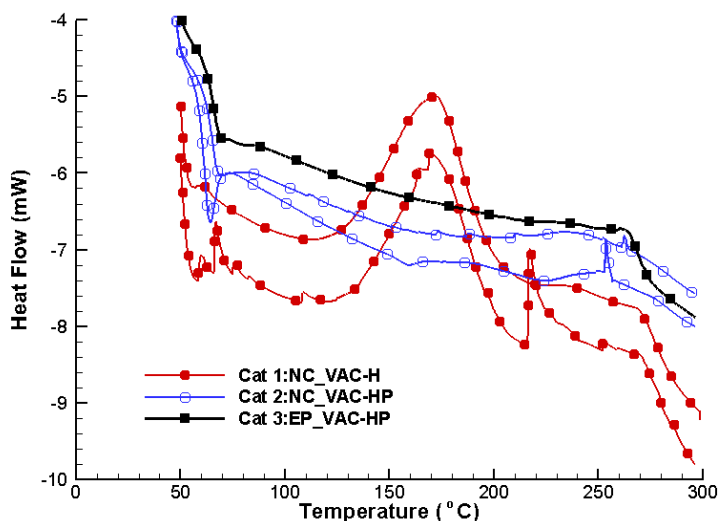
Fig. 5. DSC results for pure epoxy and CNF/epoxy specimens using both methods
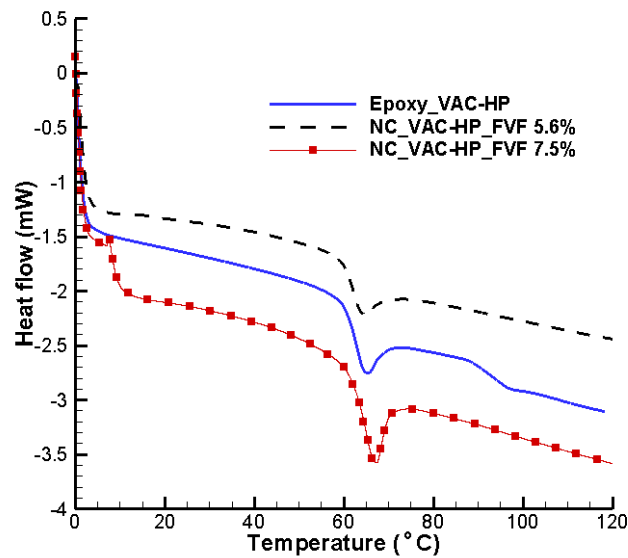
Fig. 6. DSC results for pure epoxy and CNF/epoxy specimens using VAC-HP at low temperatures

The results of dynamic mechanical analysis (DMA) are shown in Fig. 7. Figure 7(a) shows an increase in the storage modulus for the nanocellulose-reinforced samples in the glassy state. The increase was directly proportional to the amount of nanocellulose reinforcement. A similar trend was seen for the elastic modulus, as characterized by the three-point bending tests, where a 15% increase in elastic modulus was observed. At room temperature, DMA results showed an 18% increase in the storage modulus for the highest fiber volume fraction (FVF) of nanocellulose (7.5% by volume) when compared to the pure resin. As the temperature was increased, the storage modulus was highest for pure epoxy, and it decreased with increasing nanocellulose content. Figure 7(b) shows the effect of nanocellulose addition on the tan delta plots.
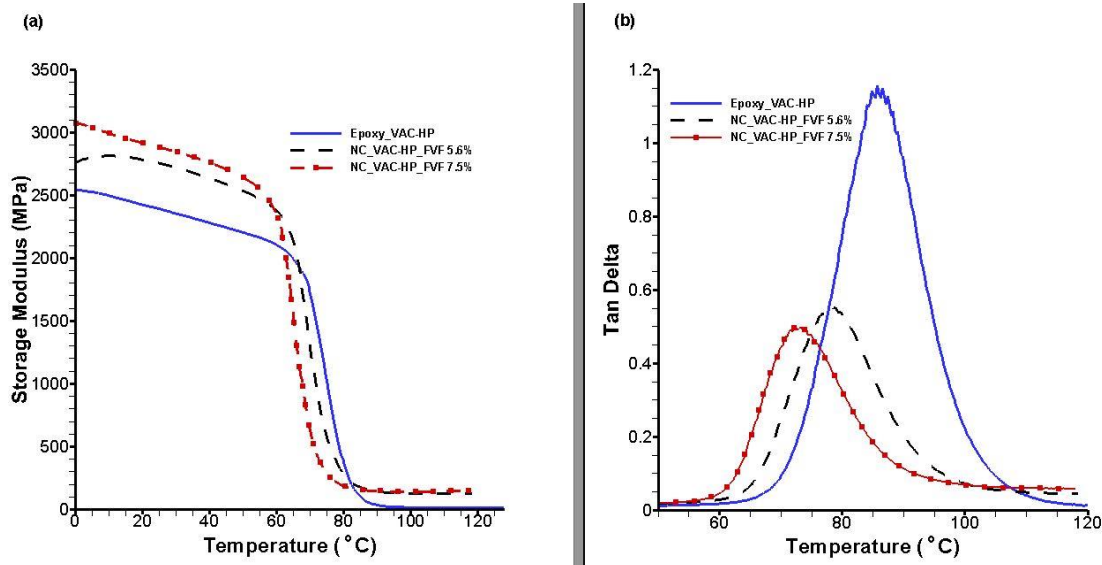
Fig. 7. DMA results for pure epoxy and CNF/epoxy specimens (prepared by VAC-HP) showing (a) storage modulus and (b) tan delta curves

The tan delta curves showed a peak shift to lower temperatures with increasing nanocellulose reinforcement. This peak shift indicated a reduction in the glass transition temperature with increasing nanocellulose content in the nanocomposites. Other studies have shown the opposite behavior, where the addition of nanocellulose increased the T_g (Jonoobi *et al.* 2010). The glass transition temperature for pure epoxy as characterized by the tan delta curves peaks was around 85 °C and dropped to 73 °C for the composite with 7.5% nanocellulose by volume. No significant changes were observed for the width of the tan delta peaks. The peak intensities were remarkably lower for the nanocellulose composites compared to neat epoxy samples. The reason for this can be attributed to the interactions between the resin and the nanocellulose, which restrict the segmental mobility of the polymer chains in the vicinity of the reinforcements (Bondeson *et al.* 2007; Jonoobi *et al.* 2010).

SEM micrographs (Fig. 8) of epoxy and CNF/epoxy composites samples showed a more ductile failure of the neat resin specimens when compared to those reinforced with nanocellulose. The CNF/epoxy samples showed a more brittle failure and the appearance of various sized voids on the fracture surface. This observation agrees with the behavior shown by the mechanical testing results (Fig. 4), for which a lower strain-to-failure was seen for the CNF/epoxy composites prepared by the VAC-HP method. Inspection of the cross-sections of the fracture surfaces of the CNF/epoxy composites also showed only a partly uniform composite, in which some areas had more cellulose and others had more resin. The presence of voids in the CNF composites and the lower strain-to-failure of the cellulose microfibrils may explain why the mechanical strength was not significantly increased by the addition of cellulose reinforcement. The voids in the microstructure could prevent the nanocellulose from adequately bonding with the epoxy and developing full strength.
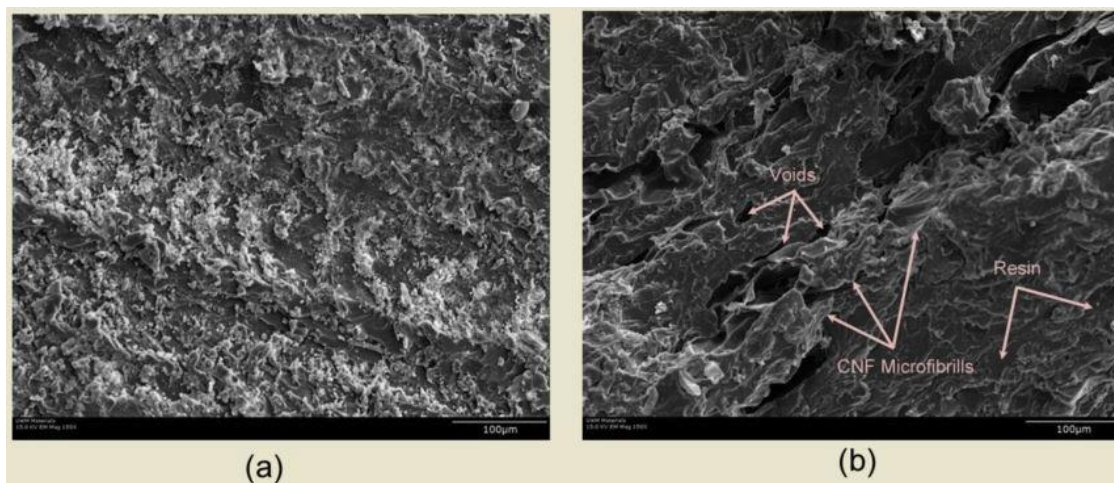
Fig. 8. SEM micrographs for (a) neat epoxy and (b) CNF/epoxy with fiber volume fraction of 5.6%

CONCLUSIONS

1. The reinforcement potential of novel nanocellulose-based reinforcements in the form of three-dimensional scaffolding was demonstrated. The success of the proposed VAC-HP in liquid mold processing is dependent on a low-viscosity epoxy (*e.g.*, 65 cPs) that can be used in liquid forming processes.

2. Nanocellulose scaffolds can be processed into composites using the proposed VAC-HP method and a low-viscosity epoxy resin, resulting in improved modulus and lower strain-to-failure compared to the neat epoxy specimens.

3. The DSC characterization of room temperature-cured resin showed that the incorporation of nanocellulose materials can result in an exothermic peak at 170 °C; this observation suggested an alteration of the curing kinetics compared to pure resin specimens. This was confirmed with mechanical testing, which showed that specimens with this exothermic peak corresponded to significantly lower mechanical properties. The exothermic peaks were eliminated with the VAC-HP method.

4. Results of the mechanical testing indicated an increase in the elastic modulus of the nanocellulose/epoxy composites prepared by the VAC-HP method by an average of 15% compared to the neat resin at reinforcement levels of 5.6 to 7.5% by weight.

5. This increase was also seen in the analysis of the viscoelastic properties using DMA, where a 14 to 18% increase in the storage modulus at room temperature was seen for these two reinforcement levels. The increase in the mechanical properties was only seen in the glassy state of the composites, and the behavior was reversed at temperatures higher than the glass transition temperature.

6. DMA results also revealed a decrease in the glass transition temperature with the addition of nanocellulose reinforcement and a decrease in the tan delta peaks.

ACKNOWLEDGMENTS

REFERENCES CITED

ASTM. (2007). "D5023 - 07 Standard Test Method for Plastics: Dynamic Mechanical Properties: In Flexure (Three-Point Bending),"

ASTM. (2010). "D790 - 10 Standard Test Methods for Flexural Properties of Unreinforced and Reinforced Plastics and Electrical Insulating Materials,"

ASTM. (2012). "D4065 - 12 Standard Practice for Plastics: Dynamic Mechanical Properties: Determination and Report of Procedures,"

Azeredo, H. M. C. D. (2009). "Nanocomposites for food packaging applications," *Food Res. Int.* 42(9), 1240-1253.

Bondeson, D., Syre, P., and Niska, K. O. (2007). "All cellulose nanocomposites produced by extrusion," *J. Biobased Mater.Bioenerg.* 1(3), 367-371.

Iwamoto, S., Nakagaito, A. N., and Yano, H. (2007). "Nano-fibrillation of pulp fibers for the processing of transparent nanocomposites," *Appl. Phys. A-Mater.Sci. Proc.* 89(2), 461-466.

Iwamoto, S., Nakagaito, A. N., Yano, H., and Nogi, M. (2005). "Optically transparent composites reinforced with plant fiber-based nanofibers," *Appl. Phys. A-Mater.Sci. Proc.* 81(6), 1109-1112.

Jonoobi, M., Harun, J., Shakeri, A., Misra, M., and Oksman, K. (2009). "Chemical composition, crystallinity, and thermal degradation of bleached and unbleached kenaf bast (*Hibiscus cannabinus*) pulp and nanofibers," *BioRes* 4(2), 626-639.

Jonoobi, M., Harun, J., Mathew, A. P., and Oksman, K. (2010). "Mechanical properties of cellulose nanofiber (CNF) reinforced polylactic acid (PLA) prepared by twin screw extrusion," *Compos. Sci. Technol.* 70(12), 1742-1747.

Masoodi, R., Elhajjar, R. F., Pillai, K. M., and Sabo, R. (2012). "Mechanical characterization of cellulose nanofiber and bio-based epoxy composite," *Mater. Design* 36(0), 570-576.

Moon, R. J., Martini, A., Nairn, J., Simonsen, J., and Youngblood, J. (2011). "Cellulose nanomaterials review: Structure, properties and nanocomposites," *Chem.Soc. Rev.* 40(7), 3941-94.

Nakagaito, A. N., and Yano, H. (2008). "The effect of fiber content on the mechanical and thermal expansion properties of biocomposites based on microfibrillated cellulose," *Cellulose* 15(4), 555-559.

Nogi, M., Handa, K., Nakagaito, A. N., and Yano, H. (2005). "Optically transparent bionanofiber composites with low sensitivity to refractive index of the polymer matrix," *Appl. Phys.Lett.* 87(24), 243110.

Nogi, M., Abe, K., Handa, K., Nakatsubo, F., Ifuku, S., and Yano, H. (2006). "Property enhancement of optically transparent bionanofiber composites by acetylation," *Appl. Phys. Lett.* 89(23),233123.

Nogi, M., Ifuku, S., Abe, K., Handa, K., Nakagaito, A. N., and Yano, H. (2006). "Fiber-content dependency of the optical transparency and thermal expansion of bacterial nanofiber reinforced composites," *Appl. Phys.Lett.* 88(13), 133124.

Nogi, M., and Yano, H. (2008). "Transparent nanocomposites based on cellulose produced by bacteria offer potential innovation in the electronics device industry," *Adv. Mater.* 20(10), 1849-1852.

Nogi, M., Iwamoto, S., Nakagaito, A. N., and Yano, H. (2009). "Optically transparent nanofiber paper," *Adv. Mater.* 21(16), 1595-1598.

Nogi, M., and Yano, H. (2009). "Optically transparent nanofiber sheets by deposition of transparent materials: A concept for a roll-to-roll processing," *Appl. Phys. Lett.* 94 (23), 233117.

Okahisa, Y., Yoshida, A., Miyaguchi, S., and Yano, H. (2009). "Optically transparent wood–cellulose nanocomposite as a base substrate for flexible organic light-emitting diode displays," *Compos. Sci. Technol.* 69(11-12), 1958-1961.

Pääkkö, M., Ankerfors, M., Kosonen, H., Nykänen, A., Ahola, S., Österberg, M., Ruokolainen, J., Laine, J., Larsson, P. T., Ikkala, O., and Lindström, T. (2007). "Enzymatic hydrolysis combined with mechanical shearing and high-pressure homogenization for nanoscale cellulose fibrils and strong gels," *Biomacromolecules* 8(6), 1934-1941.

Qing, Y., Sabo, R., Wu, Y., and Cai, Z. (2012). "High-performance cellulose nanofibril composite films," *BioResources* 7(3), 3064-3075.

Qing, Y., Sabo, R., Zhu, J.Y., Agarwal, U., Cai, Z., Wu, Y. (2013). "A comparative study of cellulose nanofibrils disintegrated via multiple processing approaches," *Carbohydr. Polym.* 97, 226-234.

Ruiz, M. M., Cavaille, J. Y., Dufresne, A., Gerard, J. F., and Graillat, C. (2000). "Processing and characterization of new thermoset nanocomposites based on cellulose whiskers," *Compos. Interfaces* 7(2), 117-131.

Sabo, R., Seo, J.-H., and Ma, Z. (2012). "Cellulose nanofiber composite substrates for flexible electronics," *2012 TAPPI International Conference on Nanotechnology for Renewable Materials*, Montreal, Quebec, Canada.

Saito, T., Hirota, M., Tamura, N., Kimura, S., Fukuzumi, H., Heux, L., and Isogai, A. (2009). "Individualization of nano-sized plant cellulose fibrils by direct surface carboxylation using TEMPO catalyst under neutral conditions," *Biomacromolecules* 10(7), 1992-1996.

Sehaqui, H., Ezekiel Mushi, N., Morimune, S., Salajkova, M., Nishino, T., and Berglund, L. A. (2012). "Cellulose nanofiber orientation in nanopaper and nanocomposites by cold drawing," *ACS Appl. Mater. Interfaces* 4(2), 1043-1049.

TAPPI. (1998). "TAPPI Test Method T237 cm-98 Carboxyl content of pulp," TAPPI Test Methods, Technical Association of the Pulp and Paper Industry, Atlanta, GA.